A survey on modeling and control of thruster-assisted position mooring systems

Roger Skjetne[a,b,c], Zhengru Ren[a,c,*]

[a]*Department of Marine Technology, Norwegian University of Science and Technology (NTNU), NO-7491 Trondheim, Norway*
[b]*NTNU, Centre for Autonomous Marine Operations and Systems (NTNU AMOS)*
[c]*Centre for Research-based Innovation on Marine Operations (SFI MOVE)*

Abstract

This review presents a systematic summary of the state-of-the-art development of technological solutions, modeling, and control strategies of thruster-assisted position mooring (TAPM) systems. The survey serves as a starting point for exploring automatic control and real-time monitoring solutions proposed for TAPM systems. A brief historical background of the mooring systems is given. The kinematics and a simplified kinetic control-design model of a TAPM system are derived in accordance with established control methods, including a quasistatic linearized model for the restoring and damping forces based on low-frequency horizontal motions of the vessel. In addition, another two mooring line models, i.e., the catenary equation and the finite element method model, are presented for the purpose of higher-fidelity simulations. The basic TAPM control strategies are reviewed, including heading control, surge-sway damping, roll-pitch damping (for semisubmersibles), and line break detection and compensation. Details on the concepts of setpoint chasing for optimal positioning of a vessel at the equilibrium position are discussed based on balancing the mooring forces with the environmental loads and avoiding mooring line failure modes. One method for setpoint chasing is the use of a structural reliability index, accounting for both mean mooring line tensions and dynamic effects. Another method is the use of a lowpass filter on the position of the vessel itself, to provide a reference position. The most advanced method seems to be the use of a fault-tolerant control framework that,

*Corresponding author
Email addresses: roger.skjetne@ntnu.no (Roger Skjetne), zhengru.ren@ntnu.no (Zhengru Ren)

in addition to direct fault detection and isolation in the mooring system, incorporates minimization of either the low-frequency tensions in the mooring lines or minimization of the reliability indices for the mooring lines to select the optimal directions for the setpoint to move. A hybrid (or supervisory switching) control method is also presented, where a best-fit control law and observer law are automatically selected among a bank of control and observer algorithms based on the supervision of the sea-state and automatic switching logic.

Keywords: Position mooring, modeling, mooring, hybrid control, optimal setpoint, fault-tolerant control.

---

1. Introduction

Stationkeeping operations are crucial to various offshore explorations, such as drilling, floating production, storage, and offloading (FPSO), and offshore installation. The main requirements for the stationkeeping operation of a floating structure are to maintain the position and heading. It influences the safety of the operators and production processes, as well as the costs of operations.

A dynamic positioning (DP) system maintains the position and heading by thrusters, and it is suitable for temporary operations in deep water. The most typical long-term stationkeeping operations are conducted using position mooring (PM) systems. Mooring lines supply restoring forces when the moored vessel drift from the equilibrium position.

An alternative modern solution is the combination of the mooring and DP systems. When Petrojarl came in 1986, the thruster-assisted position mooring (TAPM), also called posmoor, with a controlled weather-vaning capability was first introduced [1]. In addition to a typical DP function, a TAPM system also contains a mooring system, which provides passive restoring forces and moment. TAPM thus take benefits from both a passive mooring system and an active DP system. The mooring system mainly contributes to compensating the mean wave-induced or ice-induced loads, and the DP system is used as damping control for the horizontal motions and maintain the desired heading in normal seas. Hence, TAPM is a fuel-efficiency solution for long-term deepwater operations and arctic explorations.

The purpose of this survey paper is to review for the background material in the public domain on thruster-assisted, or DP-assisted, position mooring systems in the context of state-of-the-art control system solutions during the last three-four decades. Without loss of generality, the TAPM systems work for many types

of floating structures, such as FPSO and semi-submersibles. FPSOs are mainly adopted as examples to illustrate the concepts and designs. Admittedly, the references provided in this survey does not give an exhausted list. But it is believed to contain many important studies in the academic domain.

The survey is organized as follows. Section 2 briefly introduces the historical development of several mooring systems and the TAPM systems. In Section 3, the kinematic and kinetic models of a TAPM system are reviewed. Moreover, the mooring line models are introduced. The basic and more advanced control modes and strategies are described in Section 4. The paper is summarized in Section 5.

2. Historical developments of mooring solutions

The first FPSOs were converted trading tankers with a fully passive single-point mooring (SPM) system attached or incorporated to the bow or stern of the vessel, starting with the Shell Castellon built in Spain in 1977 [1, 2]. These SPM systems have a natural weather-vaning capability. Several solutions are listed as examples:

- CALM (Catenary Anchor Leg Mooring): The most elementary SPM, consisting of a floating moored buoy to which the vessel is moored using a hawser arrangement; see Figure 1(a). The hawser is connected to a turntable on the buoy to allow the vessel to weather-vane freely. Typically, it is used as a temporary loading/offloading terminal for tankers.

- SBS (Single Bouy Storage): A bouy mooring system with a triangular-shaped rigid arm connected to the turntable on top of the buoy, and with its base connected to the ship by means of hinges to allow relative pitching motions between the tanker and bouy. This has been applied for permanently moored storage tankers and for FPSO systems.

- SALM (Single Anchor Leg Mooring): As for the CALM, this consists of a bouy, but with a single anchor leg, shown in Figure 1(b). It prevents collision damages to the fluid swivels by placing them underwater and below the keel level of the tanker [3]. It is used in shallow water.

- SALS (Single Anchor Leg Storage): Type of SALM, but it is specially designed for offloading, where its behavior does not depend (almost) on the water depth due to the special anchoring system.

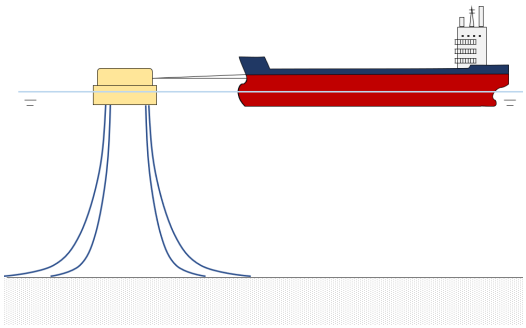

(a) CALM

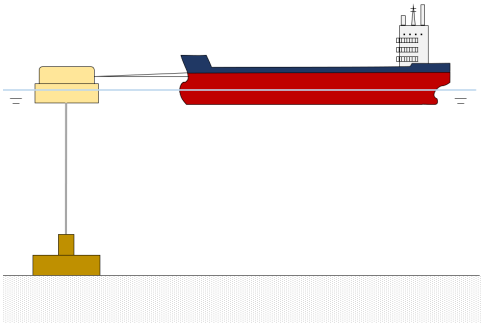

(b) SALM

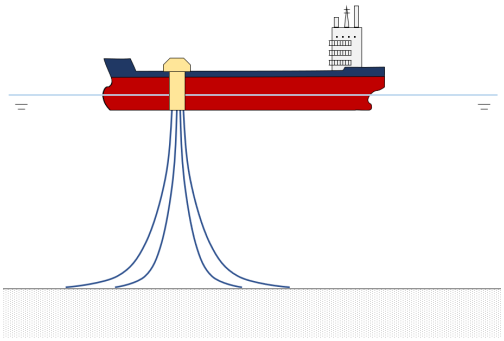

(c) Internal turret

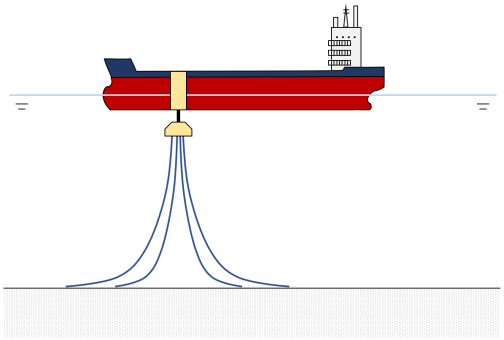

(d) BTM

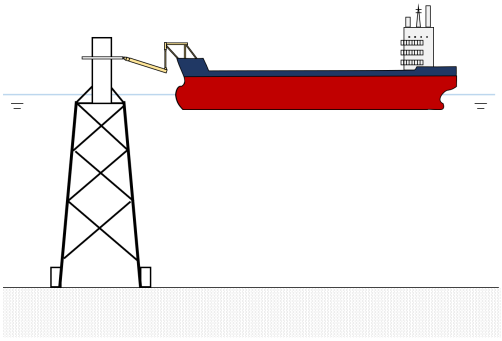

(e) Soft yoke mooring system

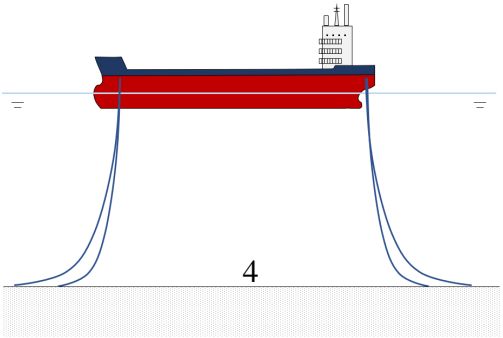

(f) Spread mooring

Figure 1: Different mooring systems.

Moving from the SPM solutions, the next development was to attach the mooring structure directly to the bow or stern of the vessel using a turret. A fully passive turret assembly is integrated into a vessel and moored by mooring lines. A bearing system allows the vessel to rotate around the turret. The turret can be attached to the bow of the vessel (external turret mooring system) or integrated into the hull structure (internal turret mooring system); see Figure 1(c).

According to De Boom [4], the first turret of this "relatively simple concept" was the stern-mounted turret mooring system for a mooring tanker rebuilt into a floating storage and offloading (FSO) unit installed on the Rospo Mare field offshore Italy in March 1987. The first turret-based mooring system of a different kind, however, was the Jabiro disconnectable riser turret mooring (RTM) system installed in 1986 for the Jabiro field in the Timor Sea, North of Australia. Since this field is exposed to tropical cyclones, it was advantageous to reduce the design levels of the vessels by implementing a disconnectable turret to be able to move away from the vessel in case of an approaching cyclone. Developed in the late 1980s, another disconnectable mooring system is the buoyant turret mooring (BTM) system, shown in Figure 1(d). The buoy supports the mooring lines and risers when the buoy disconnects with the turret, and it is locked into the receptacle at the bottom of the turret. A disconnectable turret solution was also proposed by De Boom [4] for offshore arctic operations in ice-covered Arctic waters where "a tanker may have to leave the site because of approaching icebergs", a highly relevant concept in development of Arctic offshore activities.

The development then went to constructing new-built vessels with a large diameter (up to $20\,\mathrm{m}$) internal turret for deep water to allow a large number of risers to be connected. In this case, the vertical motions of the vessel are important, implying a location of the turret closer to midship where the motions are smallest. However, if placed too close to the midship, the vessel will lose its natural weather-vaning ability. On this issue, De Boom [4] concluded that a position between $10\% - 25\%$ of ship length from bow is adequate to reduce vertical motions and maintain weather-vaning. However, for large-diameter turrets, the design of the mechanical component assuring free weather-vaning is a particular challenge. From this year new-built FPSOs were constructed with an internal turret at approximate 1/3 vessel length from the bow.

FPSOs are typically designed either with the accommodation block aft and turret at the bow, or with accommodation block fore in front of or behind the turret. Some advantages of placing the turret in the bow part, with the accommodation at stern are good natural weather-vaning ability and reduced motions at the accommodation due to the smaller vertical movements at stern compared to the bow.

Placing the accommodation in the bow with the turret behind it, has the advantage of reduced riser dynamics since the turret is closer to midship. However, the accommodation unit in front of the turret, in the bow, results in a large wind area and may deteriorate weather-vaning ability and require active heading control. According to Aalbers et al. [1], the natural weather-vaning ability is preserved with the turret positions up to 30-35% of ship length from the bow. However, the further distance the turret is placed from the bow, the larger the heading fluctuations become, resulting in increased environmental loads on the vessel. As a consequence, a study reported by [1] showed that the mooring line tensions could increase up to 150%. This is particularly problematic in shallow waters. In deeper waters, on the other hand, the mooring line tensions do not necessarily increase for more aftward turret positions if heading stability is preserved. In fact, the dynamic forces on the mooring lines tend to decrease due to the smaller vertical motions in this case. Consequently, the static/dynamic mooring line tension depends strongly on the combination of mooring line configuration, turret location, and water depth.

Several other SPM solutions exist (e.g., single anchor leg mooring rigid arm (SALMRA), articulated loading platform (ALP), soft yoke system (Figure 1(e))), and the reader is referred to [3] and [5] for better explanations and illustrations. For more details of mooring systems, details of mooring equipment, configurations, and operations, the reader is referred to the lecture presentations by Larsen [6]. Figure 2 gives an illustration of the mooring concept development.

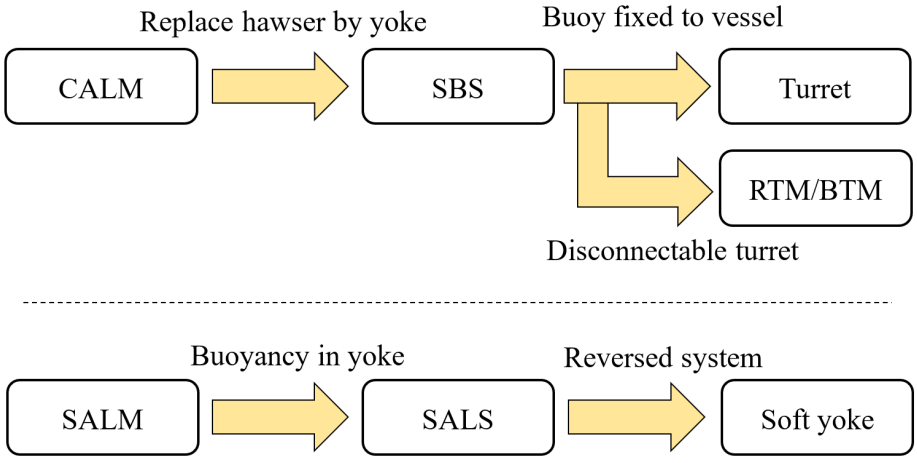

Figure 2: Historical developments of single-point mooring systems (Adapted from [5]).

The capacities of a classic passive mooring system are limited by the structural design. The moored vessel reacts to the external loads passively, resulting in risky responses in harsh environments. Furthermore, its on-site real-time performance are neither controllable nor optimizable. Hence, automated control was proposed to improve the stationkeeping performance and safety of a classic passive mooring system by introducing thruster systems. In the Equinor Norne FPSO, as illustrated in Figure 3, the two mooring principles were combined, using thrusters to reduce the loads in the mooring cables and a fluid swivel to allow continuous fluid flow during weather-vaning. This required more advanced control techniques, leading to the thruster-assisted or DP-assisted mooring systems. In the PhD thesis by Strand [7], nonlinear control techniques were derived and presented for TAPM control systems. Based on this, Chapter 8 of his thesis presented the full-scale verification for the turret-moored Varg FPSO that was delivered to Saga Petroleum in August 1998.

Figure 3: Illustration of the Norne 6608/10 FPSO (Courtesy: Equinor).

Besides the SPM, there are multi-point mooring systems, e.g., the spread mooring system illustrated in Figure 1(f). The vessel is moored by multiple mooring lines and heads to the dominant wave direction.

3. Modeling of a position mooring system

System modeling is fundamental in model-based control designs. Using the notations and modeling framework presented by Strand et al. [8], a TAPM system with an internal turret is considered in this survey; see the Norne FPSO in Figure 3. In this section, both the kinematics and kinetics models are presented with an emphasis on the mooring system.

When constant environmental loads act on the vessel, however, the point where the mooring system balance the environmental loads shift. This point is called the equilibrium position, that is, the point where the mooring forces balance the (constant) environmental loads without use of thrusters.

In accordance with [9–12], the field zero point (FZP) is defined as the equilibrium position of the vessel body-frame in $\{\mathrm{E}\}$ when no environmental loads or thruster loads are acting on the vessel, meaning the position when the vessel is at rest and the mooring line tensions balance each other.

3.1. Kinematics

As illustrated in Figure 4, the turret is anchored by N mooring lines from the anchor points on the seabed and entering the turret through the fairlead terminal points (TP) at the bottom of the vessel. At the TPs, the anchor lines enter the turret, and the mooring forces act on the body. The turret is rotated an angle α_t about the z^b-axis in the body-fixed reference frame. This gives the four reference frames of interest, as shown in Figure 5. Hereafter, the curly brackets $\{\cdot\}$ denote coordinate systems.

- Earth-fixed frame $\{\mathrm{E}\}$: The local coordinate system located at the mean sea level with the x-axis pointing towards North (N-axis), y-axis pointing to East (E-axis), and z-axis pointing downwards (D-axis). The E-frame origin for TAPM systems is typically placed at the FZP, where the center of turret (COT) is when no environmental loads act on the vessel.

- Body-fixed frame $\{\mathrm{B}\}$: The coordinate system with an origin at a fixed center (CO) in the vessel hull, typically the CO is placed on the waterline, i.e., $(L_{pp}/2, B/2, z_{WL})$, with x^b-axis positive forward (surge), y^b-axis positive towards starboard (sway), and z^b-axis positive downwards.

- Turret-fixed frame $\{\mathrm{T}\}$: Coordinate system fixed to the turret with an origin at the COT and rotated an angle α_t relative to body x-axis.

- Reference-parallel frame $\{\mathrm{D}\}$: Desired earth-fixed reference frame located at the mean sea level with origin at a desired position (x_d, y_d) and rotated to a desired heading angle ψ_d.

Note that the superscript T denotes vector decomposition in the coordinate system $\{\mathrm{T}\}$, while $\top$ denotes vector or matrix transpose.

Considering only the horizontal motions, disregarding the heave, roll, pitch motions, the position and heading of the vessel in $\{\mathrm{E}\}$ are defined by $\eta := \mathrm{col}(x, y, \psi)$ where (x, y) is the horizontal position and ψ is the heading. Similarly, define u, v, and r as surge velocity, sway velocity, and yaw rate, respectively, such that $\nu := \mathrm{col}(u, v, r)$ is the corresponding 3-degree-of-freedom (DOF) velocity vector in $\{\mathrm{B}\}$. The 3DOF velocity vector of the vessel body in $\{\mathrm{E}\}$, $\dot{\eta} = \mathrm{col}(\dot{x}, \dot{y}, \dot{\psi})$, is given by the kinematic relationship

$$\dot{\eta} = R(\psi)\nu, \qquad R(\psi) = \begin{bmatrix} \cos\psi & -\sin\psi & 0 \\ \sin\psi & \cos\psi & 0 \\ 0 & 0 & 1 \end{bmatrix}, \tag{1}$$

where $R(\psi)$ is the 3DOF rotation matrix.

Based on the work by Strand et al. [8], we give notations for the mooring system. According to Figure 6, the tangential mooring line force is denoted by T with a horizontal component H.

The length along the line from TP to the touchdown point on the seabed is denoted by the suspended length L_s, and L_{tot} is the total length of the line. D is the water depth, l_h is the horizontal length between TP and the touchdown point, and L_h is similarly the horizontal length from the TP to the anchor point.

Let $p^E_{tp,i} = (x^E_{tp,i},\ y^E_{tp,i})$ be the position of the i'th terminal point TP$_i$ in $\{\mathrm{E}\}$. If the terminal points are located on a circle of radius r_i and angle γ_i with respect to the COT, the constant position of TP$_i$ in $\{\mathrm{T}\}$ is

$$p^T_{tp,i} = \begin{bmatrix} x^T_{tp,i} \\ y^T_{tp,i} \end{bmatrix} = r_i \begin{bmatrix} \cos\gamma_i \\ \sin\gamma_i \end{bmatrix}. \tag{2}$$

Let $p^B_{cot} = (x^B_{cot},\ y^B_{cot})$ be the constant position of the COT in $\{\mathrm{B}\}$. This gives TP$_i$ in $\{\mathrm{B}\}$ as

$$p^B_{tp,i} = p^B_{cot} + R_2(\alpha_t)p^T_{tp,i} \tag{3}$$

where

$$R_2(\alpha_t) = \begin{bmatrix} \cos\alpha_t & -\sin\alpha_t \\ \sin\alpha_t & \cos\alpha_t \end{bmatrix} \tag{4}$$

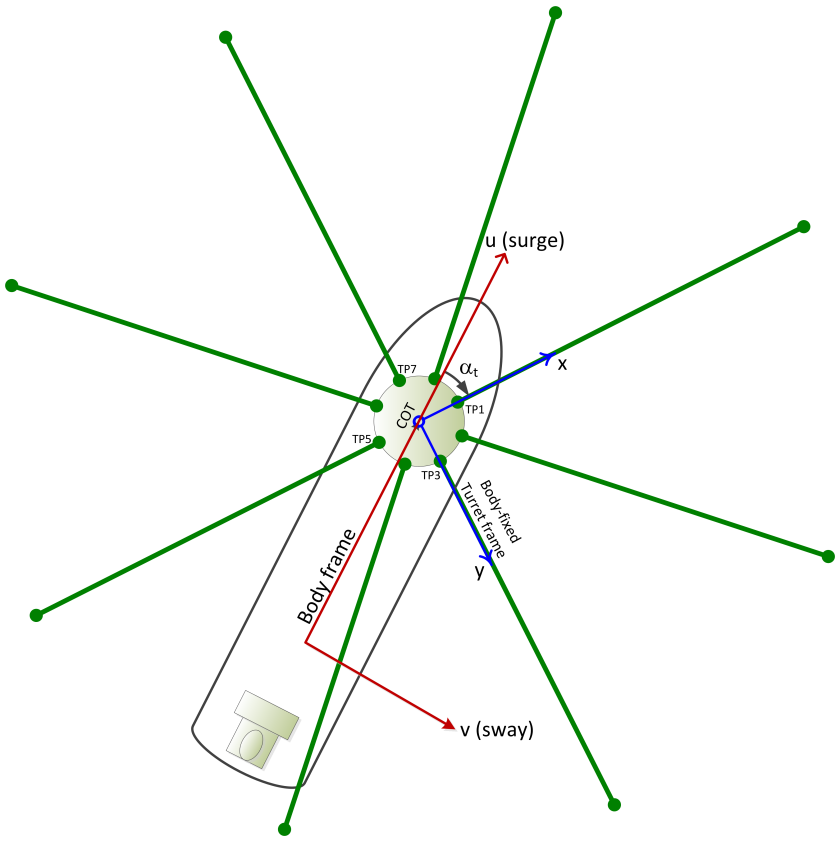

Figure 4: Illustration of the vessel body frame, the turret frame with an angle of rotation α_t, and a typical symmetric mooring configuration.

is the 2×2 rotation matrix. Letting $p^E = (x^E, y^E) = (x, y)$ be the position of the vessel body-frame in $\{\mathrm{E}\}$, the corresponding TP_i position in $\{\mathrm{E}\}$ becomes

$$\begin{aligned} p^E_{tp,i} &= p^E + R_2(\psi) p^B_{tp,i} \\ &= p^E + R_2(\psi) p^B_{cot} + R_2(\psi) R_2(\alpha_t) p^T_{tp,i} \\ &= p^E + R_2(\psi) p^B_{cot} + R_2(\psi + \alpha_t) p^T_{tp,i} \end{aligned} \tag{5}$$

or written out on scalar form,

$$p^E_{tp,i} = \begin{bmatrix} x^E + x^B_{cot} \cos\psi - y^B_{cot} \sin\psi + x^T_{tp,i} \cos(\psi + \alpha_t) - y^T_{tp,i} \sin(\psi + \alpha_t) \\ y^E + y^B_{cot} \cos\psi + x^B_{cot} \sin\psi + x^T_{tp,i} \sin(\psi + \alpha_t) + y^T_{tp,i} \cos(\psi + \alpha_t) \end{bmatrix}. \tag{6}$$

The geometric equations are obviously simplified if one chooses the COT as origin also for the body-frame, such that $p^B_{cot} = 0$ and $p^E_{tp,i} = p^E + R_2(\psi + \alpha_t) p^T_{tp,i}$.

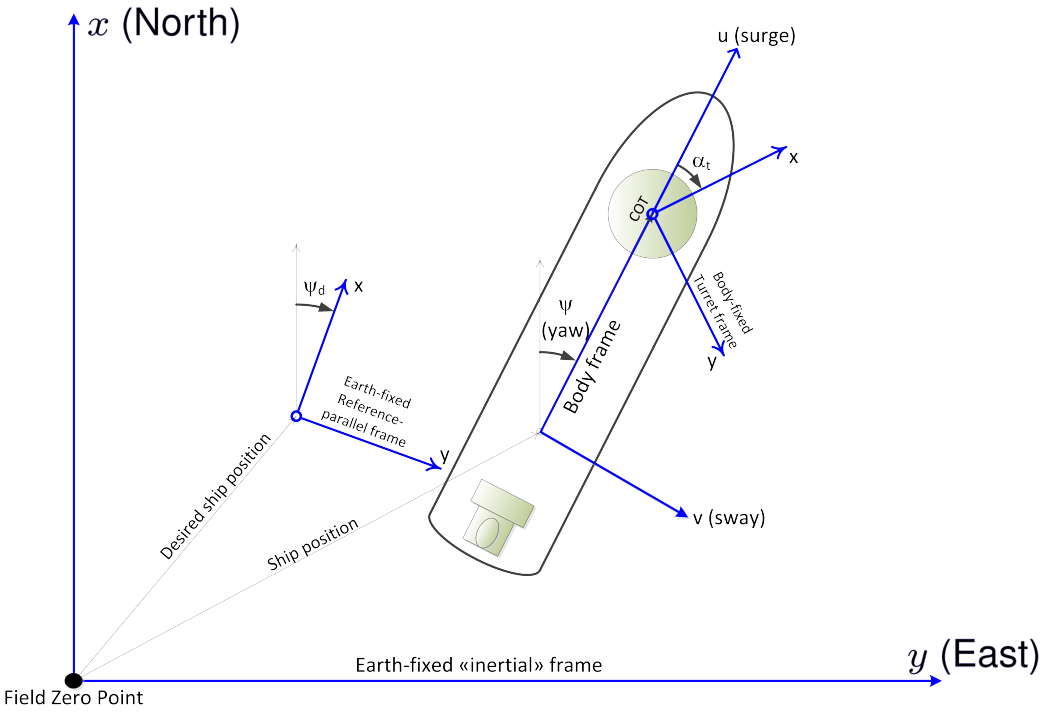

Figure 5: Definition of reference frames. (E: Earth-fixed reference frame, B: Body-fixed reference frame, and T: Turret-fixed reference frame.)

If we in addition assume that the turret is kept at a constant direction in $\{\mathrm{E}\}$, then $\alpha_t = -\psi$ and $R_2(\alpha_t) = R_2(-\psi) = R_2(\psi)^\top$ such that $p^E_{tp,i} = p^E + p^T_{tp,i}$.

3.2. Kinetics

For marine vessels, the motion is typically divided between the low-frequency (LF) dynamics and a wave-frequency (WF) model that are combined through a superposition. The details of the full 6DOF nonlinear model can be found in [13] and [14].

An irrotational ocean current with speed V_c and direction β_c in $\{\mathrm{E}\}$ is given by

$$v_c^E = \begin{bmatrix} V_c \cos\beta_c \\ V_c \sin\beta_c \\ 0 \end{bmatrix}. \tag{7}$$

We let the relative velocity between the vessel and the ocean fluid be $\nu_r := \nu -$

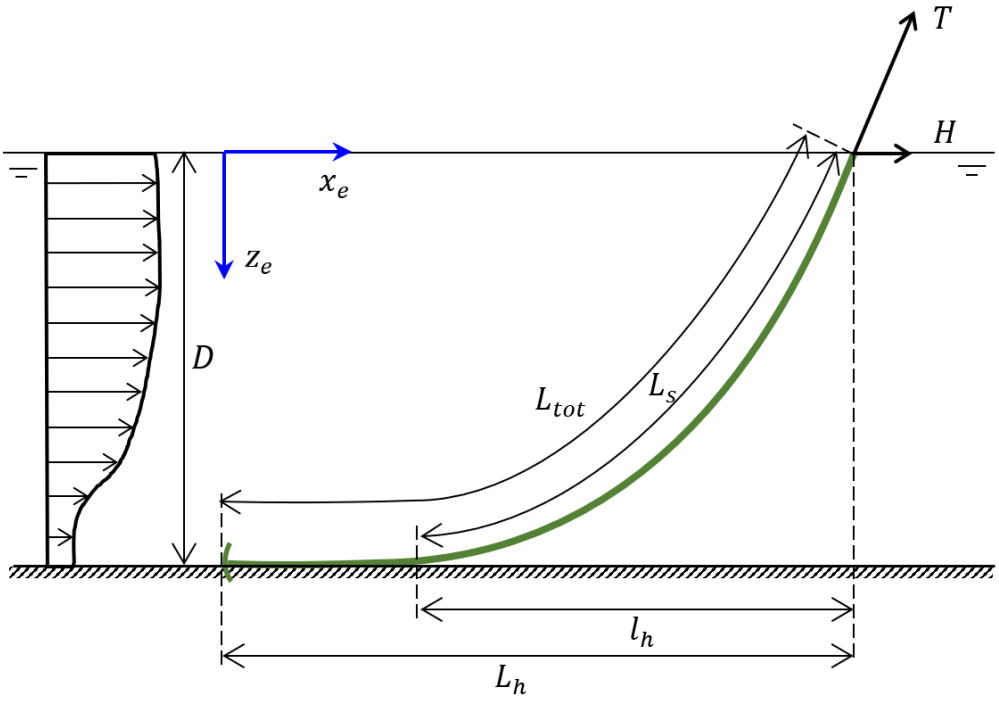

Figure 6: Profile and notations for a mooring line (Adapted from [8]).

$\nu_c = (u - u_c, v - v_c, r)$, where the irrotational ($r_c = 0$) current velocity in $\{\mathrm{B}\}$ is

$$\nu_c = R(\psi)^\top v_c^E = \mathrm{col}(u_c, v_c, 0).$$

This gives the LF model

$$M_{rb}\dot{\nu} + M_a\dot{\nu}_r + C_{rb}(\nu)\nu + C_a(\nu_r)\nu_r + D(\nu_r)\nu_r = \tau_{env} + \tau_{moor} + \tau_{thr}, \quad (8)$$

where M_{rb} and M_a are the rigid-body inertia and added mass matrices, respectively, $C_{rb}(\nu)$ and $C_a(\nu_r)$ are the rigid-body and added-mass induced Coriolis matrices, respectively, and $D(\nu_r)$ is the nonlinear damping matrix. The right-hand side environmental loads τ_{env} are due to are the wind loads τ_{wind} and 2nd-order wave drift loads τ_{wave2}, that is,

$$\tau_{env} = \tau_{wind} + \tau_{wave2}. \quad (9)$$

The loads from the mooring lines are given by τ_{moor}, while the thruster forces and moment are given by τ_{thr}. From Property 8.1 in Fossen [13, Section 8.3], when the ocean current is constant and irrotational, we have

$$M_{rb}\dot{\nu} + C_{rb}(\nu)\nu = M_{rb}\dot{\nu}_r + C_{rb}(\nu_r)\nu_r. \quad (10)$$

This gives

$$M\dot{\nu}_r + C(\nu_r)\nu_r + D(\nu_r)\nu_r = \tau_{env} + \tau_{moor} + \tau_{thr}, \quad (11)$$

where $M = M_{rb} + M_a$ and $C(\nu_r) = C_{rb}(\nu_r) + C_a(\nu_r)$.

For the 3DOF low-speed control application, it is common to assume that $C(\nu_r)\nu_r \approx 0$ and $D(\nu_r)\nu_r \approx D_{lin}\nu_r = D_{lin}\nu - D_{lin}\nu_c$. This gives two options for LF control models:

1. Using ν_r as the velocity state, we must also change (1) such that

$$\dot{\eta} = R(\psi)\nu_r + v_c^E \quad (12)$$

$$M\dot{\nu}_r + D_{lin}\nu_r = R(\psi)^\top b(t) + \tau_{wind} + \tau_{moor} + \tau_{thr}, \quad (13)$$

   where the constant current v_c^E enter as a constant perturbation in the kinematic equation, and the bias force $b(t)$ in $\{\mathrm{E}\}$ models $R(\psi)^\top b(t) \approx \tau_{wave2}$.

2. Using the absolute velocity ν as the velocity state, we get

$$\dot{\eta} = R(\psi)\nu \quad (14)$$

$$M\dot{\nu} + D_{lin}\nu = R(\psi)^\top b(t) + \tau_{wind} + \tau_{moor} + \tau_{thr}, \quad (15)$$

   where the bias force $b(t)$ in $\{\mathrm{E}\}$ now models $R(\psi)^\top b(t) \approx D_{lin}\nu_c + \tau_{wave2}$.

In the following, we will derive the mooring loads τ_{moor}, consisting of a restoring term and a damping term, that is

$$\tau_{moor} = g_{moor} + d_{moor}. \tag{16}$$

From a control perspective, there are many papers providing modeling of a TAPM system. An important starting point is the works by Strand et al. [8, 15] (including some approximations based on [16]), establishing important notations and a problem formulation for the TAPM control problem. In these papers and in [7, 17], control models applicable for model-based control design are deduced. Simple relationships for this are included in [18] using linear-spring model and [8, 17] using catenary equations. Disregarding the dynamics of the mooring lines and the influence of the current flow along with the water depth (current profile), a lookup table of a mooring line can be generated offline to simulate the mooring restoring forces. The catenary equation describes the geometric shape that a hanging chain or cable takes under influence by gravity and supported only at its end points [19]. The catenary equation can be solved by iterate binary search.

A more advanced finite element method (FEM) model of a mooring line was proposed by Aamo and Fossen [20], Sørensen et al. [21], Aamo and Fossen [22], and Fang [23]. Aamo and Fossen [22] discussed the global existence and uniqueness of solutions of a simplified fully dynamic FEM model of the mooring lines. A mooring line is discretized into a number of mass nodes that are connected to its closed two neighbor nodes. The bottom node is fixed on the seafloor, and the top end node is fixed at its corresponding TP. The positions of the nodes are firstly initialized by the catenary equation offline. The acceleration and velocity of a node update online considering the total force acting on the center of mass, including gravity, buoyancy, damping force, elastic restoring force, and current loads calculated by the Morison equation. The result is a coupled dynamic model for the vessel and the mooring system. A simulation-based analysis shows significant differences in accuracy between the dynamic model and a quasistatic model. As stated, a quasistatic model is typically adequate for shallow-water operations but gives insufficient accuracy for mooring in deep water. The comparison of different simulation models are summarized in Table 1.

Some available software packages for TAPM systems are summarized as follows. The Mimosa for mooring systems is a module of the DNV GL Sesam software which calculates the LF and WF motion of a moored vessel, as well as the mooring line tensions [24]. Developed by Marin [25], aNyMOOR.DYNFLOAT is part of the aNyMOOR suite, and it can simulate the turret and spread moored

Table 1: Comparison of mooring line modeling methods.

Method	**Linear spring**	**Catenary equation**	**FEM**
Moving region	Near the design point	Water surface	Water surface
Winch control	No	Lack of mooring line dynamics	Yes
Current profile	No	No	Yes
Computational speed	High	Medium	Low
Fidelity	Low	Medium	High

floating vessel. The updated version of MarIn toolbox [26] contains the necessary modules to simulate the turret dynamics and mooring lines for the purpose of control design. Besides, position-based dynamics method [27] is similar to the FEM model.

235 *3.2.1. Mooring line restoring forces*

From Figure 6 we get for Line i that the horizontal force H_i is directed from the anchor point $p^E_{a,i} = (x^E_{a,i},\ y^E_{a,i})$ to the corresponding terminal point $p^E_{tp,i} = (x^E_{tp,i},\ y^E_{tp,i})$ by the angle β_i with respect to the North-axis, as shown in Figure 7. This gives

$$\beta_i = \arg\left(p^E_{tp,i} - p^E_{a,i}\right) = \arctan\left(\frac{y^E_{tp,i} - y^E_{a,i}}{x^E_{tp,i} - x^E_{a,i}}\right). \tag{17}$$

From Line i, in $\{\mathrm{E}\}$ we then get the force vector

$$h_i = \begin{bmatrix} h_{x,i} \\ h_{y,i} \end{bmatrix} = \begin{bmatrix} H_i \cos\beta_i \\ H_i \sin\beta_i \end{bmatrix}, \tag{18}$$

that the vessel induces on the mooring line at TP_i. Note that the force induced by the mooring line onto the vessel is in the opposite direction.

With reference to Figure 7, we can express the corresponding load vector in the body-frame in two alternative ways. In the first method, we rotate h_i to $\{\mathrm{B}\}$ and calculates the corresponding force and moment components that h_i induces on the vessel in the body frame. Let $g^B_{mo,i}$ be the mooring force and moment for

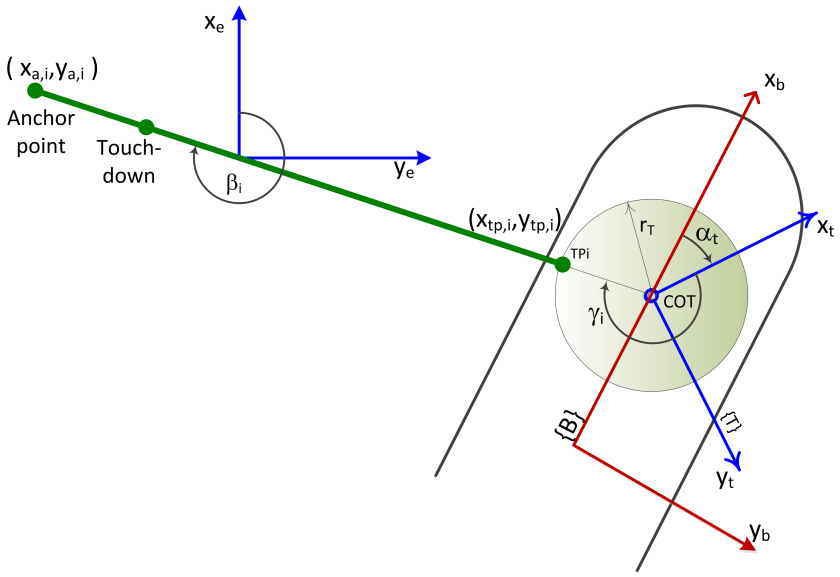

Figure 7: Notations for a single catenary mooring line.

Line i in $\{\mathrm{B}\}$. Then we get

$$
\begin{aligned}
g^B_{mo,i}(h_i,\psi,\alpha_t) &= \begin{bmatrix} -R_2(\psi)^\top h_i \\ -p^B_{tp,i} \times R_2(\psi)^\top h_i \end{bmatrix} = \begin{bmatrix} -1 & 0 \\ 0 & -1 \\ y^B_{tp,i} & -x^B_{tp,i} \end{bmatrix} R_2(\psi)^\top h_i \\
&= \begin{bmatrix} -h_{x,i}\cos\psi - h_{y,i}\sin\psi \\ -h_{y,i}\cos\psi + h_{x,i}\sin\psi \\ h_{y,i}\left(y^B_{tp,i}\sin\psi - x^B_{tp,i}\cos\psi\right) + h_{x,i}\left(y^B_{tp,i}\cos\psi + x^B_{tp,i}\sin\psi\right) \end{bmatrix}
\end{aligned} \tag{19}
$$

and g_{moor} becomes

$$
g_{moor} = \sum_{i=1}^{N} g^B_{mo,i}(h_i,\psi,\alpha_t). \tag{20}
$$

In the second method we first derive the mooring force and moment components in $\{\mathrm{E}\}$. Correspondingly, let $g^E_{mo,i}$ be the mooring force and moment for Line i in

$\{\mathrm{E}\}$. This gives

$$g^E_{mo,i}(h_i,\psi,\alpha_t) = \begin{bmatrix} -h_i \\ -\left(p^E_{tp,i} - p^E\right) \times h_i \end{bmatrix} = \begin{bmatrix} -h_i \\ -R_2(\psi)p^B_{tp,i} \times h_i \end{bmatrix} \tag{21}$$

$$= \begin{bmatrix} -1 & 0 \\ 0 & -1 \\ \bar{y} & -\bar{x} \end{bmatrix} \begin{bmatrix} h_{x,i} \\ h_{y,i} \end{bmatrix}$$

$$g^B_{mo,i}(h_i,\psi,\alpha_t) = R(\psi)^\top g^E_{mo,i}(h_i,\psi,\alpha_t), \tag{22}$$

where $\bar{y} = y^E_{tp,i} - y^E$ and $\bar{x} = x^E_{tp,i} - x^E$. The total restoring force is a superposition of all mooring lines. Then g_{moor} becomes

$$g_{moor} = \sum_{i=1}^{N} g^B_{mo,i}(h_i,\psi,\alpha_t) = R(\psi)^\top \sum_{i=1}^{N} g^E_{mo,i}(h_i,\psi,\alpha_t). \tag{23}$$

To get a quasistatic approximation for h_i, it is common to assume that the line tension T and its horizontal component H are superpositions of static terms $\bar{T}$ and $\bar{H}$ and dynamic terms δ_T and δ_H, respectively, such that

$$T = \bar{T} + \delta_T, \qquad H = \bar{H} + \delta_H. \tag{24}$$

The static forces are found from the line characteristics based on the geometric configuration of the line. The line characteristics are typically given as a function of the distance between the anchor and terminal points, that is,

$$\bar{T} = f_T(L_h), \qquad \bar{H} = f_H(L_h), \tag{25}$$

where $L_h := \left|p^E_a - p^E_{tp}\right|$. The details on this is found in [28]. The line characteristics can be linearized around a working point L_{h0} according to

$$\bar{H} = \bar{H}_0 + \left.\frac{df_H(L_h)}{dL_h}\right|_{L_h=L_{h0}} \Delta L_h, \qquad \bar{H}_0 := f_H(L_{h0}). \tag{26}$$

Letting $p^E_{tp,i,0}$ denote the nominal position of TP_i in $\{\mathrm{E}\}$ (with COT colocated with the FZP). The linearization for Line i is done at $L_{h0,i} := \left|p^E_{tp,i,0} - p^E_{a,i}\right|$ such that

$$\bar{H}_i = \bar{H}_i(p^E_{tp,i}) = \bar{H}_{0,i} + k_i\left(\left|p^E_{tp,i} - p^E_{a,i}\right| - \left|p^E_{tp,i,0} - p^E_{a,i}\right|\right), \tag{27}$$

where $p^E_{tp,i} = p^E_{tp,i}(\eta,\alpha_t)$. This implies that the restoring force g_{moor} is approximated as a function only of the LF position/heading of the ship, that is,

$$g_{moor} = \bar{g}_{moor}(\eta,\alpha_t), \tag{28}$$

by replacing H_i by $\bar{H}_i$ in (18).

Sørensen et al. [17] assumed that fixed anchor line length and that the current profile does not influence the line profile. In this case, (16) can be approximated by a 1st-order Taylor expansion of the quasistatic restoring mooring force (28) and about the working point $\eta = \eta_0$ (where the COT is colocated with the FZP). This gives the linearized restoring loads

$$g_{moor} \approx \bar{g}_{moor}(\eta_0, \alpha_t) - R(\psi)^\top G_{mo}(\eta - \eta_0). \tag{29}$$

3.2.2. Mooring line damping forces

An earlier traditional assumption of TAPM systems was that the contribution of mooring line drag in the total surge damping was negligible. However, Huse and Matsumoto [29] showed that the damping of the mooring structure actually makes out the significant damping in the total ship-mooring system. They came to the conclusions:

- For a moored ship in irregular waves, the damping of the mooring structure makes out up to 80% of the total low-frequency surge damping.
- The superimposed WF motions onto the LF motions of the vessel increases the LF surge damping due to the mooring system by a factor of 2-4.

Triantafyllou et al. [30] followed up this study and concluded that:

- The mooring lines are subject to three types of excitations: 1) Large amplitude LF motions; 2) Medium amplitude WF motions; 3) Small amplitude, very high-frequency vortex-induced vibrations.
- Mooring line damping is very important and of similar amplitude as wave drift damping. It was found that *"neglecting the drag amplification causes underprediction of the order of* 50% *in the value of the mooring line damping coefficient"*.
- Since a mooring system provides low natural periods, of the order of 100 seconds, LF excitations such as wave drift forces and unsteady wind forces, may excite resonant oscillations of significant amplitudes: *"At resonance the maximum amplitude motion, and peak slowly-varying mooring forces, are primarily controlled by damping"* [30].

As noted by Huse and Matsumoto [29], the wave-induced motions of the vessel can significantly increase the horizontal damping for the vessel. Hence, it is the absolute horizontal velocity of the vessel that induces this drag effect. Typically, this is also represented in the literature by a linear model, obtained by approximating (16) by a 1st-order Taylor expansion of d_{moor} about the working point $\nu = 0$. This gives

$$d_{moor} \approx -D_{mo}\nu. \tag{30}$$

An illustrative explanation is provided by Larsen [6] on this phenomenon.

3.3. Resulting model

It is common to use the FZP as the origin of the NED-frame $\{\mathrm{E}\}$, such that $\eta_0 = 0$. Using the absolute velocity ν as the velocity state and utilizing the simplifications, we arrive at the model

$$\dot{\eta} = R(\psi)\nu, \tag{31a}$$

$$M\dot{\nu} + D\nu + R(\psi)^\top G_{mo}\eta = \tau_{thr} + R(\psi)^\top b(t) + \tau_{wind} + \bar{g}_{moor}(0, \alpha_t), \tag{31b}$$

where $D := D_{lin} + D_{mo}$, and the bias force $b(t)$ in $\{\mathrm{E}\}$ models $R(\psi)^\top b(t) \approx D_{lin}\nu_c + \tau_{wave2}$. This could also include $\bar{g}_{moor}(0, \alpha_t)$, which in the symmetric case sums to zero. However, since it in the asymmetric case does not sum to zero (e.g. due to line break), we choose to keep $\bar{g}_{moor}$ explicit.

4. Control strategies

4.1. Overview

Equation (31) acts as a starting point of most studies. It is in strict-feedback form with unknown external disturbances [31]. System (31) has a similar form to the typical state space equation of a DP system. Therefore, relevant DP control algorithms can be adjusted to TAPM easily. However, the control strategies are different due to the fundamental distinction in the control objectives by the employment of the mooring system. The mooring system provides passive restoring force and reduces the power consumption by the thruster systems, making TAPM systems more energy efficient. The analysis by Jenssen [32] illustrated the importance of including the mooring dynamics into the DP control system for a TAPM solution, either moored to seabed, moored to another stiffly moored vessel, or moored to another DP vessel.

For a TAPM system, there are two principles as reported in [1]. The first one is to use the thruster system to produce maximum low-frequency damping

and the remaining capacity to produce restoring forces. This will position the ship at a mean excursion with small fluctuations. The second one is to use the thruster system to produce maximum restoring and remaining capacity to produce damping. This will position the ship closer to a reference point, but allows larger fluctuations.

In the control design of a TAPM system, the core problem is the tradeoff between energy consumption and operation safety (drift and line break). To improve fuel efficiency, a maximized usage of the mooring system is desired. The major approach to ensure the system reliability is to restrict the displacement in the horizontal plane. In practice, these two targets conflict with each other. Hence, the control objectives are differentiated between operation modes and various environmental conditions.

Heading control is the first priority to keep an optimized heading angle with carefully selected restoring and damping gains. Thereafter, one should apply the remaining thrust capacity on surge control, under a lower priority, with mainly restoring gains [1].

Instead of keeping at a fixed location, TAPM systems are allowed to run inside a safe region, a safety circle centered at the FZP; see the green zone in Figure 8. Inside this, the probability of line break is minimal, while outside there is an unacceptable risk of a line break in the mooring system. In addition to the mooring system, the other core components, such as riser and drill, may break when the vessel drifts away from the safe region. The thruster system only provides additional damping when the floating structure stays in a safe region in calm and normal seas. To save fuel, the thruster usage should be minimized within the safety limit, while outside the safety limit thrust must be used to bring the vessel back in and maintain a position within the safety circle. It may be necessary to also define an intermediate yellow alert zone. The thruster system gives extra restoring force to guarantee the structural and operational safety in extreme seas. An improper heading may increase wave loads acting on the vessel, resulting in growing power consumption to the power supply system.

It is also possible to increase the restoring forces by using stronger mooring cables. However, a heavy mooring system requires extra costs on material and displaces the vessel further, which may cause negative effects on vessel payloads and other challenges.

In this section, a number of control strategies are reviewed to fulfill each specific control objective in different weather conditions. We consider four basic control modes in a TAPM system, i.e., heading control, surge-sway damping control, roll-pitch control, and line break detection and compensation. Advanced

functionalities are the extensions of the basic control modes. The advanced functionalities are setpoint chasing, fault-tolerant control, hybrid control, and active tension control. Besides, mooring tension measurements can be used in position estimation. Experimental setup of a TAPM systems can be achieved by hybrid model testing [33, 34].

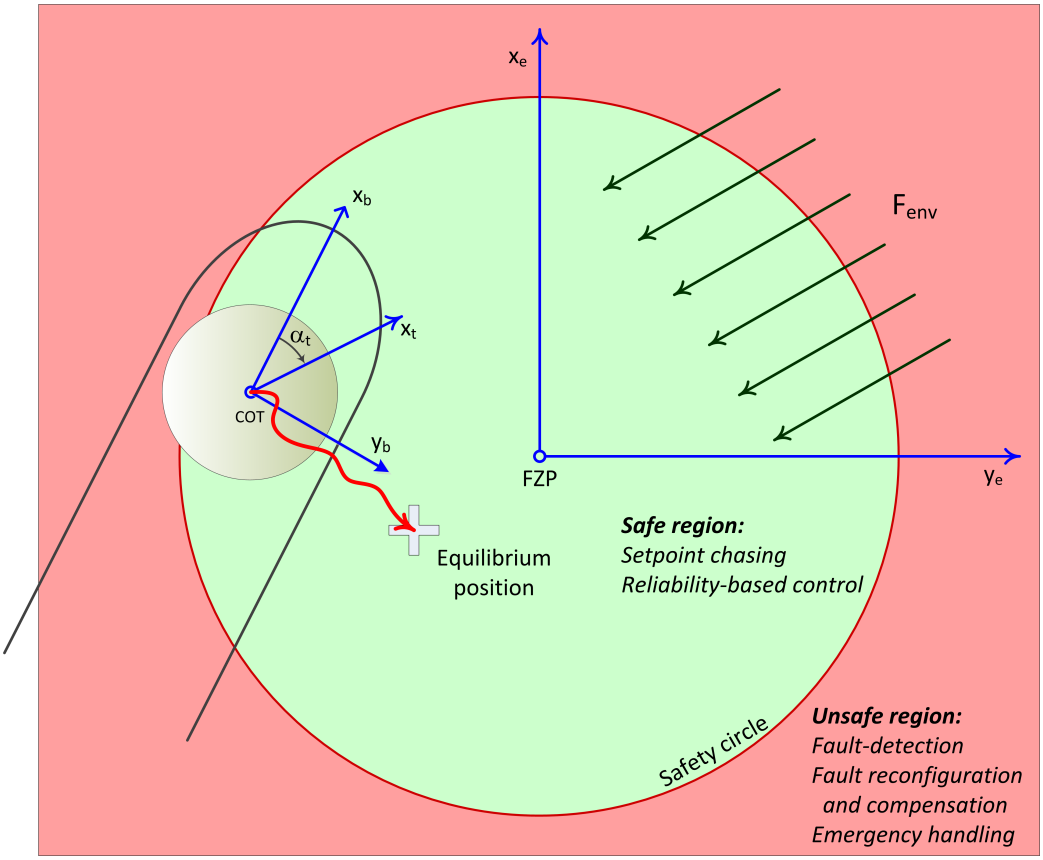

Figure 8: Safe positioning strategies for a thruster-assisted TAPM system.

4.2. Basic control modes

4.2.1. Heading control

The primary control target is to maintain the vessel at an optimal heading with limited drift loads. Heading control is essential for the performance of TAPM. For non-colinear environmental loads, heading control can be difficult, since large waves may enter from an oblique angle and push the heading from its equilibrium.

Rapid changes in yaw can deteriorate the platforms performance in surge and sway, resulting in large power consumption.

Typical proportional-integral-derivative (PID) regulation of the vessel heading (yaw) to a setpoint heading minimizes the external environmental loads on the TAPM vessel. With the turret located ahead of midship, the earth-fixed location of the turret is the DP reference point, and the vessel CG should be controlled on a circle around the turret point. Heading should be controlled such that the vessel centerline points towards the turret equilibrium point [1]. Strand et al. [8] and Sørensen et al. [17] proposed restoring, damping, and integral control (e.g., PID) to actively control the vessel heading to a desired heading against the mean environmental loads. Integral control is the negative feedback using integral action in the control loop to slowly reduce the mean steady-state offset to zero. As an alternative to integral action on the position offset, Aalbers et al. [1] proposed using a Kalman filter to predict the mean environmental forces and use this signal as feedforward.

A more advanced version is the automatic weather-vaning (weather-optimal positioning control [35, 36]), where either the optimal desired heading is automatically estimated through the environmental loads on the vessel or by controlling the vessel in the environmental force field to mimic a pendulum in a gravity field such that the heading is automatically maintained at the most favorable direction.

4.2.2. Surge-sway damping control

Instead of keeping the vessel exactly at a point, damping control plays an important role in the TAPM system, i.e., negative feedback from velocities (surge-sway or yaw rate) of a TAPM vessel to damp out oscillatory motions. The position is allowed to move in a safe region. Damping control in surge and sway is proposed by Strand et al. [8], Sørensen et al. [17] to dampen unwanted large oscillatory motions and thus reduce stress on the mooring system.

4.2.3. Roll-pitch damping control

In normal seas, only the horizontal-plane stationkeeping control is of concern in the control design. However, undesired roll-pitch oscillations may occur due to thruster usage in combination with the mooring system due to the coupled surge and pitch motions. Hence, large roll and pitch oscillations appear in high seas for floating structures with small water-plane areas, such as semi-submersibles. According to [37], the roll-pitch modes have natural periods within the bandwidth of the horizontal positioning controller. The roll-pitch damping is then added to

the typical PID controller to reduce the amplitudes of roll and pitch motions in high seas.

4.2.4. Line break detection and compensation

The vital failure of the mooring system is the mooring line break, which results in the loss of restoring force, degrades the system performance, and leads to safety threats and even hazards. A mooring line breaks for a number of reasons, such as corrosion, over limit tensile stress, and fatigue. Corrosion is not the concern in this review. The safe circle is determined to avoid the maximum limit stress. The fatigue effect is improved by changing the setpoint. Line break detection algorithms are a prerequisite [8, 38]. When a line break is detected, the thrusters must be used in feedforward to compensate for the lost mooring force.

4.3. Setpoint chasing

Setpoint chasing denotes the automatic generation of new position setpoints for the TAPM vessel in varying environmental conditions in order to find the optimal equilibrium position in which the mooring loads and environmental loads are in balance. There are a few approaches to generate the setpoints, considering the fuel consumption and structural safety of the riser and the mooring system. This will minimize thruster usage and maximize the utilization of the passive mooring. Improved restoring control with respect to the position setpoint will reduce oscillatory motions through a proportional controller. The influences of setpoints were studied in Wang et al. [39].

4.3.1. FEM-based setpoint calculation

The optimal setpoint can be calculated based on the rigid vertical components, e.g., drill string and risers. According to Sørensen et al. [21], "the most limiting operational factor in drilling is the tolerance for riser angle deviation relative to the wellhead at the top joint. Ideally, the angle should be within $\pm 2\,^{\circ}$. Deviations larger than 5-8° may be fatal." Hence, the authors proposed setpoint chasing to reduce riser angle offsets and bending stresses. This is achieved by recalculating new incremental DP setpoints based on a simplified FEM of the riser and minimizing a loss function corresponding to the lower and upper riser angles [21, 40].

An FEM model of a riser is derived, and it is shown for the purpose of calculating the top and bottom riser angles that a less accurate FEM with a maximum of 10 elements gives sufficient accuracy.

The derived dynamic LF riser model is first simplified into a quasistatic tension beam by neglecting the inertial and damping forces, and further simplified by

neglecting the influence from riser velocity. The end angle varieties are assumed to be proportional to the displacement of the moored vessel. A quadratic loss function is proposed.

The dynamic WF riser model is simplified by assuming constant system matrices and further by lineraizing the nonlinear drag forces. For setpoint chasing, the simplified LF riser model, meaning only the riser stiffness matrix, are used for explicitly calculating the new optimal incremental setpoints.

The idea is similar to the recently popular topic - digital twin. However, the unknown underwater environment involves difficulties in practical applications. The current loads acting on the riser deform it. The deformation can be considerable due to the integrated current loads in deep waters. Without underwater measurements, it is impossible to estimate the angle accurately.

4.3.2. Reliability-based control

Considering the safety of the mooring system, reliability-based control methods using the structural reliability index were studied [41, 42]. Structural reliability index, an online index $\delta_k(t)$ accounting for the breaking probability of the mooring line, is estimated for each mooring line based on the intelligent filtering of the tension measurements [43]. Letting δ_s be a lower threshold, $\delta_k(t) < \delta_s$ implies a high probability of line failure [41]. The reliability indices are directly incorporated into the control law of TAPM systems to automatically adjusts the admissible region for the moored structure in varying environmental condition and to ensure that the worst (lowest) reliability index stays above the minimum threshold, i.e., $\min(\delta_k(t)) \geq \delta_s$.

Based on the mooring line failure, the reliability index is expressed in terms of the tension by

$$\delta_k(t) = \frac{T_{b,k} - k_k\sigma_k - T_k(\mu_{k,LF}(t))}{\sigma_{b,k}}, \qquad k = 1, \ldots, N, \tag{32}$$

where $T_{b,k}$ is the mean breaking strength, σ_k is the standard deviation (STD) of the low- and high-frequency variation of the tension, k_k is a scaling factor, $T_k(\mu_{k,LF})$ is the LF mooring tension, and $\sigma_{b,k}$ is the STD of the mean breaking strength. Given the worst case (smallest) reliability index over q time instants,

$$\delta_j(t) := \min_{k\in\{1,\ldots,q\}} \delta_k(t), \tag{33}$$

the control objective is formulated to control $(\nu, \psi, \delta_j) \to (0, \psi_s, \delta_s)$. However, as pointed out by the authors, controlling $\delta_j \to \delta_s$ does not make sense in the case for

environmental conditions where $\delta_j(t) > \delta_s$, since then the thrusters would work against the mooring system and use unnecessary energy. Hence, a modification is suggested such that the reliability-based position controller is only activated when needed. Another application of the reliability-based control of moored structures can be found in [44].

In addition to the structural reliability, power consumption can be integrated into the overall optimization. Leira et al. [42] investigated the use of structural reliability criteria incorporated into the control law for TAPM systems based on the minimization of a loss function, of which two types are generally analyzed and compared. The first is quadratic in thrust force to minimize fuel consumption, and in static response to minimize offset, that is,

$$L(\mu) = K_T F_T^2 + K_F \mu^2, \tag{34}$$

where F_T is thruster force and μ is the mooring displacement. The second loss function is based on the reliability index,

$$\delta(t) = \frac{T_{b,k} - T_k(\mu_k(t)) - g\sigma_k}{\sigma_{b,k}}, \quad i = 1, \ldots, q, \tag{35}$$

giving

$$L(\mu) = K_T F_T^2 + K_P \Phi(-\delta), \tag{36}$$

where $p_f = \Phi(-\delta)$ refers to the probability of failure, and Φ is the normal cumulative distribution function. For each of these loss functions, the desired displacement μ_d is calculated as input to a positioning control law. Generally, the δ-index-based loss function seems to allow for greater variations in offset than the quadratic loss function.

Furthermore, reliability-based control is also possible to be applied to the risers. Leira et al. [45, 46] discussed the setpoint chasing control strategy and calculation of top and bottom riser angles, and how to utilize the reliability index to calculate the respective weights in the cost functions to determine which angle to minimize. A problem in setpoint chasing for riser angle control is that minimizing the level for one angle typically implies that the other angle increases. Hence, relative weights need to be inserted in the cost function to determine which angle to prioritize. To determine the incremental changes in position/heading for the DP vessel in setpoint chasing setup, Leira et al. [45, 46] proposed a loss function based on the top and bottom angles, that is,

$$L(\alpha_{top}, \alpha_{bot}) = W_{top}\left(\alpha_{top,x}^2 + \alpha_{top,y}^2\right) + W_{bot}\left(\alpha_{bot,x}^2 + \alpha_{bot,y}^2\right), \tag{37}$$

where $\alpha_{top,x}$, $\alpha_{top,y}$, $\alpha_{bot,x}$, and $\alpha_{bot,y}$ are the components of the top and bottom angles in the x- and y-axes, respectively, and W_{top} and W_{bot} are the corresponding weights. The angular components can next be expressed by the sum of the present measured angles and the incremental angles due to an incremental change of vessel position. The incremental vessel position is next expressed in terms of influence coefficients $(c_{top,x}, c_{top,y})$ and $(c_{bot,x}, c_{bot,y})$ representing the changes of the respective angular components due to a unit change of vessel position. The influence coefficients are typically given by a numerical model of the riser, e.g. FEM, and they will typically change due to varying vessel position (nonlinear geometric characteristics of the riser), riser top tension (and possibly drilling mud weight), surface current velocity, and current profile. A reliability index monitoring (or monitoring of maximum dynamic measured angles) can be applied to determine when corrective action is needed, for instance when to update the setpoint chasing algorithm. Leira et al. [46] further explored the reliability-based control scheme for riser angle control, where the reliability indices for the top and bottom riser angles are more directly controlled. To this end, several object functions based on the reliability indices for the riser angles are explored, and explicit minima are calculated to directly provide new position setpoints "to chase" by the DP system. It is noted that positioning based solely on LF quasistatic relationships are not able to capture more dynamic effects properly. Reliability indices, on the other hand, are able to capture the dynamic responses.

4.3.3. Setpoint calculation by lowpass filter

In the works by Nguyen and Sørensen [9, 11], the main contributions are the extensions of the TAPM damping control with improved restoring and mean (integral) control. Setpoint chasing is here used by finding the equilibrium point for zero thrusts. Using setpoint chasing together with integral control will help prevent line break in extreme conditions by compensating better the mean drift forces and moving the vessel closer towards the FZP. This is achieved by calculating a critical offset radius based on the mooring line capacity, and using a safety margin, to not set the reference position outside this distance even if the equilibrium position is such calculated; see Figure 8.

Improved restoring control, given a desired position from the setpoint chasing algorithm, is used to reduce oscillatory motions by use of a P-controller that shifts the natural frequency of the moored vessel outside the frequency range of the excitation loads. The desired equilibrium setpoint position (the setpoint chasing position) is here implemented by a lowpass filter of the LF position of the vessel,

that is,

$$\dot{p}_{sp} = -\Lambda \left(p_{sp} - p \right) \tag{38}$$

where $p \in \mathbb{R}^2$ is the vessel LF position.

Moreover, based on the environmental condition, a table is proposed for when to use the different TAPM control modes defined by heading control, damping control, restoring control (P), and steady-state control (I). Restoring control denotes the negative feedback from the position or heading offset to introduce artificial stiffness to the control loop. Steady-state control, also called integral control, implies the negative feedback using integral action in the control loop to slowly reduce the mean steady-state offset to zero.

4.3.4. Other approaches

Besides, Sørensen et al. [17] mentioned advisory functions, such as Posmoor consequence analysis and Posmoor simulator, in the ABB Posmoor control system for the Varg FPSO. Imakita et al. [40] presented the IRE (Intelligent Riser Estimator) that calculates the optimal reference position for vessel to minimize riser angles - essentially a setpoint chasing reference filter, and the REAPS (Riser End Angle Positioning System) that estimates the vessel movement by the riser angle sensors, without having other position reference system available.

Due to the rapid development of neural networks and learning systems, the learning algorithms are applied to calculate the optimal setpoints, for example, trained artificial neural network [47] and reinforcement learning with a deep deterministic policy gradient approach [48]. However, the challenges are to verify the stability and robustness of these approaches.

Nonlinear control methods are applied in the setpoint chasing, e.g., finite-time control [49]. Though it theoretically provides higher convergence rate, the aggressive control algorithm demands high energy input, which conflicts with the energy-efficient objective and propeller dynamics; therefore, the finite-time control seems not suitable for TAPM control systems. Other nonlinear feedback mechanisms may, on the other hand, improve the performance compared to typical linear feedback.

An extra horizontal stiffness is added to the TAPM system with the involvement of crane operations in [50]. The crane loads τ_{crane} is here added to (31b), and the setpoint is chosen to make the lift wire vertical.

4.4. Fault-tolerant control

Modeling of structural reliability to deduce reliability indices for the mooring lines, for incorporation into the positioning control design, was provided in Leira

et al. [45], Leira et al. [46], and Berntsen et al. [41], while a structural analysis of the TAPM system with the objective of fault diagnosis and fault-tolerant control (FTC) was described by Nguyen et al. [10] and Fang and Blanke [51].

To find a fault that has occurred, this involves 1) fault detection - to decide whether a fault has occurred or not, 2) fault isolation - determine in which component or function has the fault occurred, 3) fault identification - to identify the fault candidate or type of failure mode (qualitatively), and 4) fault estimation - estimate the size of the fault (quantitatively). A detected and identified fault in the control system is handled by reconfiguring the control loop, e.g. by using alternative inputs and outputs, as well as online redesign the control law.

FTC is a separate and very important subject in thruster- and DP-aided PM control systems. Faults in the pretension or mooring line break introduce significant structural changes to the system that must be detected and handled. Line break is difficult to be observed by operator. Therefore, a variety of techniques are applied to detect the break. A detected and identified fault in the control system is handled by adapting or modifying the control parameters, without changing the structure of the control system. This was considered already by Strand et al. [8]. However, Nguyen et al. [10] proposed a formal scheme for fault detection and fault accommodation of faults in the pretension or line break of mooring lines.

A graph-based structural analysis [52] was first carried out for a TAPM system based on the Matlab toolbox SaTool [53]. Parity relations based on the available redundancies in the system are used to generate a residual vector to construct a diagnosis algorithm capable of detecting and isolating faults in the mooring system. Once a fault is detected, the control accommodation is used to make the thruster-assistance take over the loss of mooring force and keep the vessel steady.

Later, a PhD study was performed by Fang [23] on FTC for TAPM systems. The faults considered here were loss of a mooring line buoyancy element and mooring line break. This included a complete structural analysis to generate residual signals and their statistical characteristics for fault detection in the system. A setpoint chasing algorithm was employed to accommodate these faults. This was based on a FEM model of the mooring lines and a setpoint generation based on optionally minimizing the tension in the mooring lines or by minimizing an objective function based on the structural reliability indices for the mooring lines [54].

The former does not take into account the dynamic effects in the mooring lines since it is only based on the LF mooring line model. The reliability-index method, on the other hand, does handle the dynamic effects of the fluctuating mooring line tensions and, thus, gives improved fault-tolerance. Nevertheless, a challenge of

the fault tolerant control is the undefined faults. If a specific failure mode is not predefined in the algorithms, the detection algorithm may be insensitive to the failure or give faulty detection, resulting in improper reaction to the failure mode.

4.5. Hybrid control concepts

Nguyen and Sørensen [12] took the setpoint chasing design of [9, 11] a step forward by introducing a supervisory (hybrid) switching algorithm that automatically determines the current sea state, based on monitoring of the wave peak frequency and the mean environmental load. Based on a hysteresis switching logic, the best-fit model and corresponding controller is determined automatically according to Figure 9.

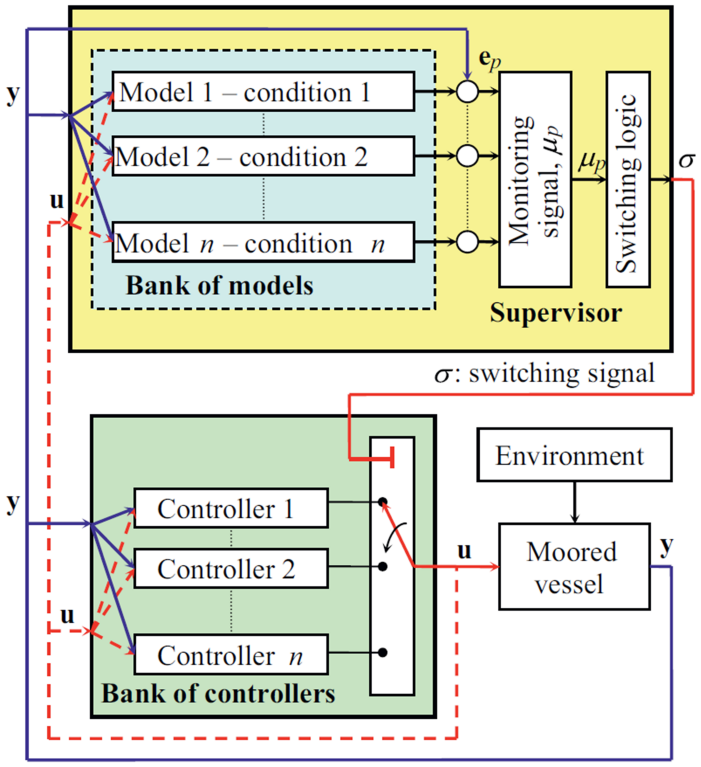

Figure 9: Supervisory switching control for a TAPM system based on sea state. (Courtesy: [12])

.

A set of control laws are proposed for heading control, surge-sway damping, surge-sway restoring and integral control, and a setpoint chasing strategy.

These control laws are tabulated in Table 2, where $H_\psi = \mathrm{diag}\,(0,0,1)$ and $H_{xy} = \mathrm{diag}\,(1,1,0)$ are projections enabling either heading or surge-sway control, respectively, and $\mathrm{Pr}_{Safe}\{\eta_{xy}\}$ is the projection of the LF position of the vessel into the safe region to minimize risk of line break. The switching of different algorithms are listed as Table 3.

Table 2: Hybrid switching.

Control actions	**Control laws**
Integral action:	$\dot{\xi} = \eta - \eta_d$
1. Heading PID control:	$\tau_{pid}^{\psi} = -H_\psi K_i R(\psi)^\top \xi - H_\psi K_p R(\psi)^\top (\eta - \eta_d) - H_\psi K_d (\nu - \nu_d)$
2. Surge-sway damping:	$\tau_d^{xy} = -H_{xy} K_d (\nu - \nu_d)$
3. Surge-sway restoring:	$\tau_p^{xy} = -H_{xy} K_p R(\psi)^\top (\eta - \eta_d)$
4. Surge-sway mean:	$\tau_p^{xy} = -H_{xy} K_i R(\psi)^\top \xi$
Setpoint normal sea:	$\dot{\eta}_r = -\Lambda \eta_r + \Lambda \eta_{xy}, \qquad \eta_{xy} = p_{LF}^E \in \mathbb{R}^2$ (see (38))
Setpoint extreme sea:	$\eta_r = \mathrm{Pr}_{Safe}\{\eta_{xy}\}$

Table 3: Hybrid switching.

Heading	**Damping**	**Restoring**	**Mean**	**Control action**	**Setpoint**	**Sea state**
✓				1		Calm
✓	✓			1+2		Normal
✓	✓	✓		1+2+3	Normal	Normal
✓	✓		✓	1+2+4	Extreme	Extreme
✓	✓	✓	✓	1+2+3+4	Extreme	Extreme

Simulations and experimental testing in NTNU Marine Cybernetics Laboratory (MCLab), carried out for the Norne FPSO, demonstrated the success of the control strategies - especially for the last approach where the switching logic automatically selected controller (without chattering) during a developing sea state condition. This was concluded to enable an increased weather window for such operations.

Mooring line failure detection and recovery can be achieved by supervisory control. In Ren et al. [38], a bank of observers was designed to estimate the moored vessel motion in different modes. The supervisor detects the mode with

the minimum residual signal and switches to the controller designed for the corresponding mode. Hassani et al. [55] solved the problem using dynamic hypothesis testing. The conditional probability of each hypothesis is calculated by running a bank of Kalman filters.

4.6. Active tension control

For a specific mooring line connecting two points in space, the restoring force at the top end increases with shortened line length. Based on such fact, active tension control of the mooring lines can be implemented by controlling the winch servo motors of the mooring lines placed on the vessel. The design target is to reduce the loads on the thrusters in stationkeeping. The motivation stems from TAPM in deeper waters where the thrusters are more used for stationkeeping, also in normal conditions, to reduce the design dimensions of the mooring system.

Based on the availability of a DP system and continuous measurements of the mooring line tensions, Aamo and Fossen [20] presented a finite-element model of the mooring lines and shows that this model is passive from the winding velocity of the tension control units to the upper end tensions. Hence, passive controllers such as P, PI, and PID can be utilized to produce the allocated winch forces. Extra care should be taken when using the control strategies. The mooring line should be controlled and, meanwhile, ensure the structural safety by limiting the winch motor rate and the tension below the moor line maximum strength.

4.7. Monitoring solutions using tension measurements

Besides the line break detection, the mooring line tension measurements are very useful to estimate the unknown anchor positions and to estimate the underwater depth-dependent current profile.

Since the tension force of a fixed-length mooring line acting on the top end is proportional to its projection distance on the seafloor, a tension measurement is transformed to a range signal using a line-of-sight assumption. Several aspects must be considered in the range signal, including the fairleads, turret dynamics, and slow-varying current profiles. An extended Kalman filter (EKF)-based simultaneous localization and mapping (SLAM) algorithm is adopted to estimate the positions of both the unknown anchors and the COT [56, 57]. Historical data are collected and enter the estimator together with the real-time measurements. The saved data of each period is considered to be a virtual vessel. The algorithm provides a redundant position reference signal to the moored structure, and it can also detect the uncertain locations of the anchors. Sensitivity studies show that the effects of the unknown underwater current are larger than the surface current.

The positioning accuracy can be improved by increasing the number of the virtual vessels.

When the positions of the mooring line anchors and bottom end of a rigid riser are known, the mooring line tensions and riser end angle can be applied to estimate the two-dimensional current profile [58]. The underwater current profile is distinguishable with these measurements. The WF motions are assumed as white noise, which is eliminated by the mean value over a period.

5. Conclusions

Technical innovations of TAPM systems in the past decades have greatly improved the energy efficiency, structural safety, and system robustness of medium-to-long-term deepwater operations. As a relative to the DP control system, the modeling and control designs of a TAPM system have a higher complexity due to the involvement of the mooring system, resulting in various levels of modeling simplification, diverse control objectives, and additional failure modes. The operational criteria vary with the working environmental conditions, projects, auxiliary components, etc. All these changes introduce significant challenges in the control design of TAPM systems. The survey presents the theoretical development, from the basic PID controller to advanced control strategies.

A simplified model of the mooring system, including the kinematics and kinetics, is presented for the purpose of control design, and high-fidelity modeling approaches are proposed to simulate the coupled TAPM system as realistic as possible. Commercial software is developed to simulate the moored vessel dynamics and conduct reliability analysis for the mooring system.

A safety region is preset to limit the motion scope of the moored structure according to the fuel consumption and structural safety. In the region, the structural reliability of the mooring system and riser system are of concern. Heading control and damping control are the fundamental functionalities of a TAPM system. In high seas, roll-pitch damping control is considered by modifying the typical feedback control law. To avoid the severe consequences of a mooring line break, detection algorithms should run in parallel.

Numerous setpoint chasing algorithms are proposed to calculate the optimized setpoint. The optimization is based on a virtual FEM model or tension measurements using the structural reliability index. Fault-tolerant control is adopted to detect the system failures and compensate for the loss of mooring force. Hybrid control using a switching logic is employed to optimize the system performance in different sea states and failure modes. Instead of controlling the DP system,

active tension control can be achieved by controlling the winch servo motor to control the restoring force provided by each mooring line.

Mooring line tension measurements is a promising supplement to typical sensor outputs. It is possible to estimate the unknown anchor positions and on-site current profile.

Acknowledgment

This work was supported by the Research Council of Norway (RCN) through the Centre of Excellence on Autonomous Marine Operations and Systems (NTNU AMOS, RCN-project 223254) and the Centre for Research-based Innovation on Marine Operations (SFI MOVE, RCN-project 237929). We also wish to thank Kongsberg Maritime AS for a good dialog on the topics presented in this paper.

References

[1] A. B. Aalbers, S. A. W. Janse, W. C. de Boom, DP assisted and Passive Mooring for FPSO's, in: Proc. Offshore Technology Conference, vol. 27, OTC, Houston, Texas, 281–288, doi:10.4043/7722-MS, 1995.

[2] Wikipedia, Floating production storage and offloading — Wikipedia, The Free Encyclopedia, URL `http://en.wikipedia.org/w/index.php?title=Floating_production_storage_and_offloading&oldid=563159034`, [Online; accessed 24-February-2020], 2020.

[3] J. Wichers, Guide to single point moorings, WMooring, 2013.

[4] W. C. De Boom, The Development of Turret Mooring Systems for Floating Production Units, in: Proc. Offshore Technology Conference, vol. 21, OTC, Houston, Texas, 201–212, doi:10.4043/5978-MS, 1989.

[5] J. Wichers, Guide to Single Point Moorings, WMooring Inc., 2013.

[6] K. Larsen, Mooring and station keeping of floating structures, Lecture, lecture notes in course TMR4225 Marine operations at NTNU, 2020.

[7] J. P. Strand, Nonlinear Position Control Systems Design for Marine Vessels, PhD thesis, Norwegian Univ. Science & Technology, Dept. Eng. Cybernetics, Trondheim, Norway, 1999.

[8] J.-P. Strand, A. J. Sørensen, T. I. Fossen, Design of automatic thruster assisted mooring systems for ships, Modeling, Identification and Control 19 (2) (1998) 61–75, doi:10.4173/mic.1998.2.1.

[9] D. T. Nguyen, A. J. Sørensen, Setpoint Chasing for Thruster-Assisted Position Mooring, in: Proc. Int. Conf. Ocean, Offshore & Arctic Eng., vol. 26, ASME, San Diego, Ca, USA, 553–560, doi:10.1115/OMAE2007-29429, 2007.

[10] D. T. Nguyen, M. Blanke, A. J. Sørensen, Diagnosis and fault-tolerant control for thruster-assisted position mooring, in: Proc. IFAC Conf. Contr. Appl. Marine Systems, vol. 7, IFAC, Bol, Croatia, ISSN 14746670, 287 – 292, 2007.

[11] D. T. Nguyen, A. J. Sørensen, Setpoint Chasing for Thruster-Assisted Position Mooring, IEEE J. Oceanic Eng. 34 (4) (2009) 548–558, ISSN 0364-9059, doi:10.1109/JOE.2009.2034553.

[12] D. T. Nguyen, A. J. Sørensen, Switching control for thruster-assisted position mooring, Contr. Eng. Practice 17 (9) (2009) 985 – 994, ISSN 0967-0661, doi:http://dx.doi.org/10.1016/j.conengprac.2009.03.001.

[13] T. I. Fossen, Handbook of Marine Craft Hydrodynamics and Motion Control, John Wiley & Sons Ltd, ISBN 9781119991496, 2011.

[14] J. A. Sørensen, Marine Control Systems: Propulsion and Motion Control of Ships and Ocean Structures, Norwegian Univ. Science & Technology, Trondheim, Norway, 2 edn., report UK-12-76, 2012.

[15] J. Strand, A. J. Sørensen, T. I. Fossen, Modelling and control of thruster assisted position mooring systems for ships, in: Proc. IFAC Conf. Manoeuvering and Contr. of Marine Crafts, vol. 4, IFAC, Brijuni, Croatia, 160–165, 1997.

[16] O. M. Faltinsen, Sea Loads on Ships and Offshore Structures, Cambridge University Press, 1990.

[17] A. J. Sørensen, J. P. Strand, T. I. Fossen, Thruster assisted position mooring system for turret-anchored FPSOs, in: Proc. IEEE Int. Conf. Contr. Appl., vol. 2, 1110–1117, doi:10.1109/CCA.1999.801128, 1999.

[18] M. Nakamura, H. Kajiwara, W. Koterayama, T. Hyakudome, et al., Control system design and model experiments on thruster assisted mooring system, in: The Seventh International Offshore and Polar Engineering Conference, International Society of Offshore and Polar Engineers, 641–648, 1997.

[19] Wikipedia, Catenary — Wikipedia, The Free Encyclopedia, URL http://en.wikipedia.org/w/index.php?title=Catenary&oldid=598709869, [Online; accessed 24-February-2020], 2020.

[20] O. M. Aamo, T. I. Fossen, Controlling line tension in thruster assisted mooring systems, in: Proc. IEEE Int. Conf. Contr. Appl., vol. 2, 1104–1109, doi:10.1109/CCA.1999.801126, 1999.

[21] A. J. Sørensen, B. Leira, J. P. Strand, C. M. Larsen, Optimal setpoint chasing in dynamic positioning of deep-water drilling and intervention vessels, Int. J. Robust Nonlinear Contr. 11 (13) (2001) 1187–1205, ISSN 1099-1239, doi:10.1002/rnc.602.

[22] O. M. Aamo, T. I. Fossen, Finite Element Modelling of Moored Vessels, Math. and Comp. Modelling Dyn. Syst. 7 (1) (2001) 47–75, doi:10.1076/mcmd.7.1.47.3632.

[23] S. Fang, Fault Tolerant Position Mooring Control Based on Structural Reliability, PhD thesis, Norwegian Univ. Science & Technology, Trondheim, Norway, 2012.

[24] D. GL, Mooring system and individual mooring line analysis - Mimosa, URL https://www.dnvgl.com/services/mooring-system-and-individual-mooring-line-analysis-mimosa-2313, [Online; accessed 24-February-2020], 2020.

[25] Marin, Assessment of a turret or spread moored FPSO: aNyMOOR.DYNFLOAT, URL https://mods.marin.nl/download/attachments/3145739/aNyMOOR-DYNFLOAT%5B1%5D.pdf?version=1{&}modificationDate=1390401490000, [Online; accessed 24-February-2020], 2020.

[26] Z. Ren, Z. Jiang, R. Skjetne, Z. Gao, Development and application of a simulator for offshore wind turbine blades installation, Ocean Engineering 166 (2018) 380–395.

[27] X. Jiang, H. Ren, X. He, Simulation of Mooring Lines Based on Position-Based Dynamics Method, IEEE Access 7 (2019) 142796–142805.

[28] K. Larsen, Static equilibrium of a mooring line, Lecture, lecture notes in course TMR4225 Marine operations at NTNU, 2020.

[29] E. Huse, K. Matsumoto, Mooring Line Damping Due to First- and Second-Order Vessel Motion, in: Proc. Offshore Technology Conference, vol. 21, OTC, Houston, Texas, 135–148, doi:10.4043/6137-MS, 1989.

[30] M. S. Triantafyllou, D. K. P. Yue, D. Y. S. Tein, Damping Of Moored Floating Structures, in: Proc. Offshore Technology Conference, vol. 26, OTC, Houston, Texas, 215–224, doi:10.4043/7489-MS, 1994.

[31] Z. Ren, B. Zhao, D. T. Nguyen, Finite-Time Backstepping of a Nonlinear System in Strict-Feedback Form: Proved by Bernoulli Inequality, IEEE Access 8 (2020) 47768–47775.

[32] N. A. Jenssen, On The Use of Safety Moorings in DP Operations, in: Dynamic Positioning Conf., Marine Tech. Soc., 2008.

[33] J. Bjørnø, H.-M. Heyn, R. Skjetne, A. R. Dahl, P. Frederich, Modeling, parameter identification and thruster-assisted position mooring of c/s inocean cat i drillship, in: ASME 2017 36th International Conference on Ocean, Offshore and Arctic Engineering, American Society of Mechanical Engineers Digital Collection, OMAE2017–61896, 2017.

[34] E. S. Ueland, R. Skjetne, S. A. Vilsen, Force actuated real-time hybrid model testing of a moored vessel: A case study investigating force errors, IFAC-PapersOnLine 51 (29) (2018) 74–79.

[35] T. I. Fossen, J. P. Strand, Nonlinear passive weather optimal positioning control (WOPC) system for ships and rigs: Experimental results, Automatica 37 (5) (2001) 701–715.

[36] Ø. K. Kjerstad, M. Breivik, Weather Optimal Positioning Control for Marine Surface Vessels, in: Proc. IFAC Conf. Contr. Appl. Marine Systems, vol. 8, IFAC, Rostock, Germany, 114–119, 2010.

[37] A. J. Sørensen, J. P. Strand, Positioning of small-waterplane-area marine constructions with roll and pitch damping, Contr. Eng. Practice 8 (2) (2000)

205 – 213, ISSN 0967-0661, doi:http://dx.doi.org/10.1016/S0967-0661(99)00155-0.

[38] Z. Ren, R. Skjetne, V. Hassani, Supervisory control of line breakage for thruster-assisted position mooring system, IFAC-PapersOnLine 48 (16) (2015) 235–240.

[39] L. Wang, J. Yang, H. He, S. Xu, T.-c. Su, et al., Numerical and experimental study on the influence of the set point on the operation of a thruster-assisted position mooring system, International journal of offshore and polar engineering 26 (04) (2016) 423–432.

[40] A. Imakita, S. Tanaka, S. Takagawa, Y. Amitani, Intelligent Riser Angle Control DPS, in: Dynamic Positioning Conf., Marine Tech. Soc., Houston, USA, 2000.

[41] P. I. B. Berntsen, O. M. Aamo, B. J. Leira, Dynamic Positioning of Moored Vessels Based on Structural Reliability, in: Proc. IEEE Conf. Decision & Control, vol. 45, IEEE, 5906–5911, doi:10.1109/CDC.2006.377085, 2006.

[42] B. J. Leira, P. I. B. Berntsen, O. M. Aamo, Station-keeping of moored vessels by reliability-based optimization, Probabilistic Eng. Mechanics 23 (23) (2008) 246 – 253, ISSN 0266-8920, doi:http://dx.doi.org/10.1016/j.probengmech.2007.12.021.

[43] H. Madsen, S. Krenk, N. Lind, Methods of structural safety, Prentice-Hall, Inc, New Jersey, USA, ISBN 0-486-44597-6, 1986.

[44] P. I. B. Berntsen, O. M. Aamo, B. J. Leira, A. J. Srensen, Structural reliability-based control of moored interconnected structures, Contr. Eng. Practice 16 (4) (2008) 495 – 504, ISSN 0967-0661.

[45] B. J. Leira, Q. Chen, A. J. Sørensen, C. M. Larsen, Modeling of Riser Response for DP Control, J. Offshore Mech. Arct. Eng. 124 (4) (2002) 219–225, doi:10.1115/1.1491274.

[46] B. J. Leira, A. J. Sørensen, C. M. Larsen, A reliability-based control algorithm for dynamic positioning of floating vessels, Structural Safety 26 (1) (2004) 1 – 28, ISSN 0167-4730, doi:http://dx.doi.org/10.1016/S0167-4730(03)00018-3.

[47] D. E. Sidarta, J. OSullivan, H.-J. Lim, Damage Detection of Offshore Platform Mooring Line Using Artificial Neural Network, in: ASME 2018 37th International Conference on Ocean, Offshore and Arctic Engineering, American Society of Mechanical Engineers Digital Collection, 2018.

[48] S. Yu, L. Wang, B. Li, H. He, Optimal setpoint learning of a thruster-assisted position mooring system using a deep deterministic policy gradient approach, Journal of Marine Science and Technology (2019) 1–12.

[49] G. Xia, C. Liu, B. Zhao, X. Chen, X. Shao, Finite Time Output Feedback Control for Ship Dynamic Positioning Assisted Mooring Positioning System with Disturbances, International Journal of Control, Automation and Systems 17 (11) (2019) 2948–2960.

[50] J. Ye, M. Godjevac, S. Baldi, H. Hopman, Joint estimation of vessel position and mooring stiffness during offshore crane operations, Automation in Construction 101 (2019) 218–226.

[51] S. Fang, M. Blanke, Fault Monitoring and Fault Recovery Control for Position-Moored Vessels, Int. J. Appl. Math. Comput. Sci. 21 (3) (2011) 467–478, doi:10.2478/v10006-011-0035-9.

[52] M. Blanke, D. T. Nguyen, Fault tolerant position-mooring control for offshore vessels, Ocean Engineering 148 (2018) 426–441.

[53] T. Lorentzen, M. Blanke, SaTool users manual, Technical Report, Automation at rsted-DTU, Technical University of Denmark, Build. 326, DK 2800 Kgs. Lyngby, Denmark, 2004.

[54] S. Fang, B. J. Leira, M. Blanke, Position mooring control based on a structural reliability criterion, Structural Safety 41 (2013) 97–106.

[55] V. Hassani, A. M. Pascoal, A. J. Sørensen, Detection of mooring line failures using Dynamic Hypothesis Testing, Ocean Engineering 159 (2018) 496–503.

[56] Z. Ren, R. Skjetne, Ø. K. Kjerstad, A tension-based position estimation approach for moored marine vessels, IFAC-PapersOnLine 48 (16) (2015) 248–253.

[57] Z. Ren, R. Skjetne, A tension-based position estimation solution of a moored structure and its uncertain anchor positions, IFAC-PapersOnLine 49 (23) (2016) 251–257.

[58] Z. Ren, R. Skjetne, An on-site current profile estimation algorithm for a moored floating structure, IFAC-PapersOnLine 49 (23) (2016) 153–158.

Appendix. Notations

The abbreviations and variables used in the present survey are listed in Table 4 and 5, respectively.

Table 4: Abbreviations in the present survey.

BTM	Buoyant turret mooring
CALM	Catenary anchor leg mooring
COT	Center of turret
DOF	Degree of freedom
DP	Dynamic positioning
EKF	Extended Kalman filter
FEM	Finite element method
FSO	Floating storage and offloading
FPSO	Drilling, floating production, storage, and offloading
FZP	Field zero point
LF	Low-frequency
MCLab	Marine Cybernetics Laboratory
PID	Proportional-integral-derivative
PM	Position mooring
RTM	Riser turret mooring
SPM	Single-point mooring
SALM	Single anchor leg mooring
SALMRA	Single anchor leg mooring rigid arm
SALS	Single anchor meg storage
SBS	Single Bouy Storage
SLAM	Simultaneous localization and mapping
STD	Standard deviation
TAPM	Thruster-assisted position mooring
TP	Terminal points
WF	Wave-frequency

Table 5: Notations in the present survey.

$\{\mathrm{B}\}$	Body-fixed frame	N	Number of mooring lines
$\{\mathrm{D}\}$	Reference-parallel frame	i, k	Index of a mooring line
$\{\mathrm{E}\}$	Earth-fixed frame	β	Mooring line lay angle
$\{\mathrm{T}\}$	Turret-fixed frame	l_h	Horizontal length between TP and touchdown point
$\mathbb{R}$	Real number	L_h	Horizontal length from the TP to the anchor point
x, y, z	Axes in $\{E\}$	L_s	Suspended length
u, v, r	Surge velocity, sway velocity, and yaw rate	L_{tot}	Total length of the line
ψ	Heading	T	Mooring line tension
x^b, y^b, z^b	Axes in $\{B\}$	δ_T	Dynamic tension
x_d, y_d, ψ_d	Desired horizontal position and heading	$\bar{T}$	Static tension
p	Horizontal position	δ_H	Dynamic horizontal force
η	Vector of horizontal position and heading	H	horizontal component of mooring line tension
η_d	Desired horizontal position and heading	$\bar{H}$	Static horizontal force
ν	3DOF velocity vector	f_H, f_T	Functions
ν_r	Relative velocity between vessel and ocean fluid	γ_i	Angle of the i'th terminal point TP_i in $\{\mathrm{T}\}$
V_c	Current speed	α_{top}, α_{bot}	Top and bottom angles
β_c	Current direction	c_{top}, c_{bot}	Change of the respective angular component
v_c^E	Constant current	d_{moor}	Damping mooring forces
D	Water depth	g_{moor}	Restoring mooring forces
$C_{rb}(\nu)$, $C_a(\nu_r)$	Rigid-body and added-mass induced Coriolis matrices	h_i	Restoring force vector in the horizontal plane
$D(\nu_r)$	Nonlinear damping matrix	r_i	Radius of turret
M_{rb}, M_a	Rigid-body inertia and added mass matrices	α_t	Rotation angle of the turret
R, R_2	3DOF and 2DOF rotation matrices	$T_{b,k}$	Mean breaking strength
τ_{env}	Environmental loads	μ	Mooring displacement
τ_{wind}	Wind loads	μ_d	Desired displacement
τ_{wave2}	2nd-order wave drift loads	L	Loss function
τ_{moor}	Loads from the mooring lines	δ_k	Index accounting for breaking probability of mooring line
τ_{thr}	Thruster forces and moment	δ_s	Lower threshold of an index
b	Bias force vector	p_f	Probability of failure
K_p, K_i, K_d	Control gain matrices	σ_k	STD of low- and high-frequency variation of the tension
K_T, K_P	Matrices	$\sigma_{b,k}$	STD of the mean breaking strength
W_{top}, W_{bot}	Weighting matrices	F_T	Thruster force